to the Robin and Day classification[26]) with substantial electron–vibrational coupling λ_0 and sufficiently low electronic coupling strength ϵ_0. The latter condition implies that the charge-transfer band at $\sim 2\epsilon_0$ should be located close to the energy range of the predicted charge-transfer-induced IR absorptions. This proximity would increase the intensity of the induced IR absorption, as indicated in (17) or (32). A system with symmetrical vibrations of high frequencies (w_α) would have large vibronic coupling (see (9) and note that $g_\alpha = \lambda_\alpha \hbar w_\alpha$) and hence would be expected to give stronger induced IR absorptions. It is of interest to note that the organic semiconductor MEM(TCNQ)$_2$, in which strong charge-transfer-induced IR absorptions are observed, possesses a charge transfer or intervalence band at ~ 3500 cm^{-1}, which is indeed very close to the induced IR absorptions (~ 2200–100 cm^{-1}).[7]

We wish to point out that the PKS model is in fact a vibronic model for a two-site, single-electron system. A similar model has recently been proposed by Rice et al.[17] to describe some dimeric organic semiconductors in which *both* the IR enhanced absorptions related to a_{1g} vibrations as well as the charge-transfer absorption have been observed. It is of great interest to be able to observe the charge-transfer-induced IR transitions in mixed-valence compounds. In this regard, Fourier transform IR spectroscopic technique should prove particularly valuable, as demonstrated by Clark and Swanson recently.[27]

Acknowledgment. It is a pleasure to thank Professor P. N. Schatz, of the Chemistry Department at the University of Virginia, for support, discussion, and useful comments on the manuscript. Special thanks go to Dr. M. J. Rice, of Webster Research Center, Xerox Corp., for sending reprints of his works and giving comments. Comments and suggestions by the reviewers are gratefully acknowledged. This work is in part supported by the National Science Foundation under Grant CHE8025608.

(26) Robin, M. B.; Day, P. *Adv. Inorg. Chem. Radiochem.* **1967**, *10*, 247–422.

(27) Clark, H. W.; Swanson, B. I. *J. Am. Chem. Soc.* **1981**, *103*, 2928.

Contribution from the Department of Chemistry, University of Alberta, Edmonton, Alberta, Canada T6G 2G2

Rh–Rh Bond Protonation in $[Rh_2Cl_2(\mu\text{-}CO)(Ph_2PCH_2PPh_2)_2]$ and the Structure of an Unusual Oxidative-Addition Product, $[Rh_2Cl_3(\mu\text{-}H)(\mu\text{-}CO)(Ph_2PCH_2PPh_2)_2]\cdot H_2O$

BRUCE R. SUTHERLAND and MARTIN COWIE*

Received December 21, 1982

The reaction of $[Rh_2Cl_2(\mu\text{-}CO)(DPM)_2]$ (DPM = $Ph_2PCH_2PPh_2$) with protonating acids, HA (A = Cl, $SO_3C_6H_4CH_3$, BF_4), yields $[Rh_2Cl_2(\mu\text{-}H)(\mu\text{-}CO)(DPM)_2(A)]$, in which protonation of the Rh–Rh bond and coordination of the A^- anion to one of the Rh centers have occurred. The products are either nonelectrolytes or weak electrolytes in CH_2Cl_2 solution. $^{31}P\{^1H\}$ and ^1H NMR spectra of these products indicate that they are symmetrical on the NMR time scale owing to fluxional processes that result either from anion dissociation and recoordination or from reversible loss of HA; in both processes the result is anion transfer from one rhodium center to the other. The BF_4^- anion in the HBF_4 adduct can be displaced by THF to yield $[Rh_2Cl_2(\mu\text{-}H)(\mu\text{-}CO)(DPM)_2(THF)][BF_4]$, which it seems has a structure similar to that of the HBF_4 adduct but with THF instead of BF_4^- coordinated to one metal. An X-ray structure determination of the HCl adduct, $[Rh_2Cl_3(\mu\text{-}H)(\mu\text{-}CO)(DPM)_2]$, confirms that the chloride ion is coordinated to one rhodium atom and that Rh–Rh bond protonation has occurred. This product has bridging hydride and carbonyl groups, two terminal chloro ligands on one metal and one on the other, and two mutually trans, bridging DPM groups. $[Rh_2Cl_3(\mu\text{-}H)(\mu\text{-}CO)(DPM)_2]$ crystallizes with one hydrogen-bound H_2O of crystallization per complex molecule in the space group $I2/a$ with $a = 25.021$ (3) Å, $b = 14.697$ (2) Å, $c = 27.486$ (3) Å, $\beta = 107.57$ (1)°, and $Z = 8$. Refinement has converged to $R = 0.052$ and $R_w = 0.058$ for 227 parameters varied and 5535 unique observed reflections.

Introduction

We have undertaken an investigation into the Rh–Rh bond protonation in $[Rh_2Cl_2(\mu\text{-}CO)(DPM)_2]$ (**1**) because of the implications regarding carbonyl activation and ligand coupling reactions. Insertion of acetylenes into the Rh–Rh bond of **1** has previously been observed to result in Rh–Rh bond cleavage and concomitant rehybridization of the carbonyl group toward sp^2 with lowering of the CO bond order.[1] This rehybridization and the movement of the metals apart also bring the carbonyl group into closer contact with the inserting group, a transformation that may lead to ligand coupling reactions. Protonation of the Rh–Rh bond in **1**, it was felt, might lead to partial rehybridization of the carbonyl group owing to lengthening of the Rh–Rh bond to a distance intermediate between those in **1** and in the acetylene-inserted product. We were interested in the possibility of stabilizing a bridging-carbonyl geometry that was intermediate between those observed at the limits of a "normal" metal–metal bond[2] and the nonbonded extreme.[1,3,4]

A comparison of the chemistry of **1** with acids having coordinating and noncoordinating anions was also of interest owing to the potential of the former to undergo oxidative-addition reactions, at either or both metal centers. In particular, the addition of HX across the Rh–Rh bond yielding a Rh(II)–Rh(II) species (viewing the CO group as a neutral one-electron donor to each metal) having a bridging CO and

(1) Cowie, M.; Southern, T. G. *J. Organomet. Chem.* **1980**, *193*, C46–C50; *Inorg. Chem.* **1982**, *21*, 246–253.

(2) Colton, R.; McCormick, M. J. *Coord. Chem. Rev.* **1980**, *31*, 1–52.

(3) Colton, R.; McCormick, M. J.; Pannan, C. D. *J. Chem. Soc., Chem. Commun.* **1977**, 823–824; *Aust. J. Chem.* **1978**, *31*, 1425–1438.

(4) Brown, M. P.; Keith, A. N.; Manojlovic-Muir, Li.; Muir, K. W.; Puddephatt, R. J.; Seddon, K. R. *Inorg. Chim. Acta* **1979**, *34*, L223–L224.

0020-1669/84/1323-1290$01.50/0

Table I. Spectral Parameters for the Compounds

no.	compd	infrared[a,b] ν(CO), cm^{-1}	infrared[a,b] ν(Rh-H), cm^{-1}	$^{31}P\{^1H\}$ NMR[b,c] δ	$^{31}P\{^1H\}$ NMR[b,c] J, Hz	^1H NMR[b,c,d,e] δ
1	$[Rh_2Cl_2(\mu\text{-}CO)(DPM)_2]$	1748 (1764)		19.8	116.0	7.78–7.11 (m, 40 H), 3.26 (m, 2 H), 3.21 (m, 2 H)
2a	$[Rh_2Cl_3(\mu\text{-}H)(\mu\text{-}CO)(DPM)_2]\cdot H_2O$	1812 (1818)	1267	21.4	95.5	7.67–7.16 (m, 40 H), 3.64 (m, 2 H), 3.41 (m, 2 H), −18.4 (m, 1 H)[d]
2b	$[Rh_2Cl_3(\mu\text{-}H)(\mu\text{-}CO)(DPM)_2]$	1809	1265	*f*		
3	$[Rh_2Cl_2(\mu\text{-}H)(\mu\text{-}CO)(DPM)_2(OSO_2C_6H_4CH_3)]$	1806 (1812)	1261	21.4	95.4	7.86–7.02 (m, 44 H), 4.92 (m, 2 H), 3.35 (m, 2 H), 2.40 (s, 3 H), −18.4 (m, 1 H)
4	$[Rh_2Cl_2(\mu\text{-}H)(\mu\text{-}CO)(DPM)_2(FBF_3)]$	1818 (1815)	1264	22.9	94.1	7.69–7.13 (m, 40 H), 3.99 (m, 2 H), 3.37 (m, 2 H), −18.9 (m, 1 H)
5	$[Rh_2Cl_2(\mu\text{-}H)(\mu\text{-}CO)(DPM)_2(THF)][BF_4]$	1785	1230	*g*		

[a] Solid-state infrared spectra were run as Nujol mulls on KBr plates. Solution values are quoted in parentheses. [b] All solution spectra were run in CH_2Cl_2 unless otherwise noted. [c] 25 °C. [d] See text for a description of the DPM methylene and the hydride resonances. [e] Abbreviations: m, multiplet; s, singlet; br, broad unresolved peak. [f] The NMR spectra of **2a** and **2b** are identical. [g] NMR spectra not obtained owing to the insolubility in THF and the deprotonation of **5** in other solvents.

no accompanying Rh–Rh bond was of interest.

The protonation of **1** using acids having coordinating and what are normally regarded as noncoordinating anions was therefore investigated, and the structure of the product of HCl addition was determined to establish the structural transformations occurring upon protonation.

Experimental Section

All solvents were appropriately dried and degassed prior to use and all reactions carried out under an atmosphere of N_2. Infrared spectra were recorded on a Nicolet 7199 Fourier transform infrared spectrometer as Nujol mulls on KBr plates or in solution between NaCl plates. $^{31}P\{^1H\}$ and ^1H NMR spectra were obtained on a Bruker HFX-90 (operating at 36.4 MHz) and a Bruker WH-400 spectrometer, respectively. The phosphorus chemical shifts were calculated relative to external H_3PO_4 and were measured by using an external deuterium lock (acetone-d_6); positive shifts are downfield from the standard. Spectral parameters for all compounds are shown in Table I. Compound **1**, $[Rh_2Cl_2(\mu\text{-}CO)(DPM)_2]$, was prepared according to the literature procedure.[5]

Preparation of Compounds. (i) $[Rh_2Cl_3(\mu\text{-}H)(\mu\text{-}CO)(DPM)_2]\cdot H_2O$ (2a). Technical grade gaseous HCl was passed through a solution of **1** (100 mg in 10 mL of THF) at a rate of ca. 0.25 mL s^{-1}. After approximately 15 s the solution turned from red-brown to bright yellow. The HCl flow was shut off after 2 min and the flask above the solution was flushed with N_2 to remove the HCl atmosphere. Addition of 30 mL of diethyl ether or 30 mL of methanol saturated with HCl yielded a red-orange powder, which was washed with several portions of diethyl ether to remove the excess HCl and dried in vacuo for several hours. The deuteride was prepared analogously by using gaseous DCl. Conductivity measurements on **2a** showed it to be nonconducting ($\Lambda(10^{-3}$ M) = 1.5 Ω^{-1} cm^2 equiv^{-1}).[6] See Table I for details of spectral characterizations of this and other compounds. Anal. Calcd for $Rh_2Cl_3O_2P_4C_{51}H_{47}$: C, 54.31; H, 4.20; Cl, 9.43. Found: C, 54.86; H, 4.21; Cl, 9.38.

(ii) $[Rh_2Cl_3(\mu\text{-}H)(\mu\text{-}CO)(DPM)_2]$ (2b). Compound **2b** was prepared as described for **2a** except that anhydrous gaseous HCl was passed through a solution of **1** in rigorously dried CH_2Cl_2. The addition of 30 mL of diethyl ether yielded a dull yellow powder, which was washed with several portions of diethyl ether and dried in vacuo. Compound **2b** was identical with **2a** in its solution properties and could be converted into **2a** by the addition of a few drops of water. Anal. Calcd for $Rh_2Cl_3OP_4C_{51}H_{45}$: C, 55.19; H, 4.09; Cl, 9.58. Found: C, 55.11; H, 3.92; Cl, 9.49.

(iii) $[Rh_2Cl_2(\mu\text{-}H)(\mu\text{-}CO)(DPM)_2(p\text{-}O_3SC_6H_4CH_3)]$ (3). Fifty milligrams of *p*-toluenesulfonic acid in 5 mL of acetone was added to a CH_2Cl_2 solution of **1** (100 mg in 5 mL). After approximately 1 h the red-brown solution had turned bright yellow. Precipitation of a bright yellow powder was induced by the addition of 30 mL of diethyl ether. The solid was collected and washed with several portions of diethyl ether to remove the excess acid and finally dried in vacuo for several hours. Conductivity measurements ($\Lambda(10^{-3}$ M) = 0.7 Ω^{-1} cm^2 equiv^{-1}, CH_2Cl_2 solution) indicated that **3** was nonconducting. Anal. Calcd for $Rh_2Cl_2O_4P_4SC_{58}H_{52}$: C, 55.83; H, 4.20; Cl, 5.68. Found: C, 55.62; H, 4.49; Cl, 5.03.

(iv) $[Rh_2Cl_2(\mu\text{-}H)(\mu\text{-}CO)(DPM)_2(BF_4)]\cdot CH_2Cl_2$ (4). Fifty microliters of $HBF_4\cdot Et_2O$ was added to a solution of **1** in CH_2Cl_2 (100 mg in 5 mL). The solution rapidly changed to bright yellow. Addition of 30 mL of diethyl ether caused the precipitation of a bright yellow microcrystalline solid, which was collected, washed with diethyl ether, and dried in vacuo. Conductivity measurements on **4** showed that this product was partially conducting in CH_2Cl_2 ($\Lambda(10^{-3}$ M) = 12.2 Ω^{-1} cm^2 equiv^{-1}), and a $^{31}P\{^1H\}$ NMR spectrum showed only the resonance due to **4**. Anal. Calcd for $Rh_2Cl_2OP_4F_4BC_{51}H_{45}$: C, 49.15; H, 3.64; Cl, 11.38. Found: C, 48.60; H, 3.73; Cl, 11.45.

(v) $[Rh_2Cl_2(\mu\text{-}CO)(DPM)_2(THF)][BF_4]\cdot THF$ (5). Fifty microliters of $HBF_4\cdot Et_2O$ was added to a suspension of 100 mg of **1** in 5 mL of THF, and the mixture was stirred vigorously for 1 h, during which time a light yellow precipitate appeared. The solid was collected, washed with Et_2O, and dried in vacuo. The conductivity of **5** ($\Lambda(10^{-3}$ M) = 16.4 Ω^{-1} cm^2 equiv^{-1}, CH_2Cl_2 solution) was significantly less than that expected for a 1:1 electrolyte;[6] however, a $^{31}P\{^1H\}$ NMR spectrum of this solution indicated that deprotonation had occurred, yielding **1** as the major phosphorus-containing species. Anal. Calcd for $Rh_2Cl_2OP_4F_4BC_{63}H_{69}$: C, 54.93; H, 5.04; Cl, 5.15. Found: C, 54.88; H, 5.10; Cl, 5.18.

X-ray Data Collection. Suitable quality, red-orange single crystals were grown by diffusion of methanol saturated with HCl into a THF solution of **2a**.

Preliminary film data showed that the crystals belonged to the monoclinic system with systematic absences (hkl ($h+k+l = 2n+1$), $h0l$ ($h = 2n+1$, $l = 2n+1$), $0k0$ ($k = 2n+1$)) characteristic of the space groups Ia and $I2/a$. These nonstandard settings of Cc and $C2/c$, respectively, were retained because of their more favorable β angle (ca. 107.6° vs. 129.9°). Accurate cell parameters were obtained by a least-squares analysis of 12 carefully centered reflections chosen from diverse regions of reciprocal space obtained with use of a narrow X-ray source. Data were collected on a Picker four-circle X-ray diffractometer equipped with a scintillation counter and a pulse height analyzer tuned to accept 90% of the Mo Kα radiation. See Table II for pertinent crystal data and the details of data collection. Absorption corrections were applied to the data by using Gaussian integration.[7]

Structure Solution and Refinement. The structure was solved in the space group $I2/a$ by using Patterson and Fourier techniques and was refined by full-matrix least-squares methods. The alternative space group, Ia, was rejected on the basis that refinement proceeded

(5) Cowie, M.; Dwight, S. K. *Inorg. Chem.* **1980**, *19*, 2500–2507.
(6) For $[Rh_2(CO)_3(\mu\text{-}Cl)(DPM)_2][BPh_4]$, which is a normal 1:1 electrolyte, $\Lambda(10^{-3}$ M) = 45.8 Ω^{-1} cm^2 equiv^{-1} in CH_2Cl_2.
(7) For programs used in the solution and refinement of the structure see ref 5.

Table II. Summary of Crystal Data and Intensity Collection

compd	$[Rh_2Cl_3(\mu\text{-}H)(\mu\text{-}CO)(DPM)_2]\cdot H_2O$
fw	1125.98
formula	$Rh_2Cl_3P_4O_2C_{51}H_{47}$
cell parameters	
a, Å	25.021 (3)
b, Å	14.697 (2)
c, Å	27.486 (3)
β, deg	107.57 (1)
V, Å^3	9636.00
Z	8
d, g cm^3	1.552 (calcd), 1.54 (1) (obsd)
space group	$I2/a$
general positions	$(0, 0, 0; \frac{1}{2}, \frac{1}{2}, \frac{1}{2}) +$ $x, y, z; \bar{x}, \bar{y}, \bar{z}; x, \bar{y}, \frac{1}{2} + z;$ $\bar{x}, y, \frac{1}{2} - z$
cryst dimens	0.016 × 0.028 × 0.030 cm
cryst shape	monoclinic prism with faces of form $\{100\}$, $\{110\}$, $\{001\}$, and $\{11\bar{2}\}$
cryst vol, mm^3	0.0094
temp, °C	22
radiation	Mo Kα (λ 0.709 300 Å); graphite monochromated
μ, cm^{-1}	10.121
range in abs cor factors	0.796–0.875
receiving aperature	5 × 4 mm; 30 cm from crystal
takeoff angle, deg	2.90
scan speed	2° in 2θ/min
scan range	0.90° below Kα to 0.90° above $K\alpha_2$
bkgd counts	20 s ($3° \leq 2\theta \leq 48°$); 40 s ($48° \leq 2\theta \leq 51°$)
2θ limits	$3° \leq 2\theta \leq 51°$
unique data used ($F_o^2 \geq 3\sigma(F_o^2)$)	5535
rinal no. of parameters refined	227
error in observn of unit wt	1.484
R	0.052
R_w	0.058

well in $I2/a$ with reasonable positional and thermal parameters, and all hydrogen atoms, except for those of the H_2O of crystallization, were located. Atomic scattering factors were taken from Cromer and Waber's tabulation[8] for all atoms except hydrogen, for which the values of Stewart et al.[9] were used. Anomalous dispersion terms[10] for Rh, Cl, and P were included in F_c. The phenyl rings were refined as rigid groups having D_{6h} symmetry and C–C distances of 1.392 Å, with each carbon atom having an independent isotropic thermal parameter. The hydrogen atoms of the DPM ligands were included, as fixed contributions, in their idealized positions with a C–H distance of 0.95 Å and isotropic thermal parameters of 1 Å^2 greater than the isotropic B (or equivalent isotropic B) of their attached carbon atom. The hydrido ligand was refined isotropically. All other non-hydrogen atoms were refined anisotropically. The final model in $I2/a$ with 227 parameters refined converged to $R = 0.052$ and $R_w = 0.058$.[11]

The final position and isotropic thermal parameters of the individually refined atoms and the phenyl carbons are given in Tables III and IV, respectively. The derived hydrogen positions and their thermal parameters, the anisotropic thermal parameters for the non-hydrogen atoms, and a listing of observed and calculated structure factor amplitudes used in the refinement are available.[12]

Discussion

The reactions of $[Rh_2Cl_2(\mu\text{-}CO)(DPM)_2]$ (**1**) with the protic acids HCl, HBF_4, and $HO_3SC_6H_4CH_3$ yield compounds in which the metals are simultaneously bridged by two DPM groups, a carbonyl group, and a hydride ligand; in other words protonation of the Rh–Rh bond in **1** has occurred in all cases. However these reactions are not merely protonation reactions since the anions of the above acids also become involved in coordination to the metals, as will be discussed separately for each reaction (vide infra). Nevertheless, the spectral parameters for all compounds obtained (see Table I) suggest similar structures for these species. The carbonyl stretching frequencies, ranging from 1785 to 1818 cm^{-1}, suggest normal bridging-carbonyl moieties, and the metal hydride stretches, between 1230 and 1267 cm^{-1}, are also typical of bridging hydrides.[13] Confirmation of the assigned metal–hydride stretches is obtained by reaction of **1** with DCl, which yielded the Rh–D stretch at 890 cm^{-1} giving a ν(Rh–H)/ν(Rh–D) ratio of 1.42, close to the expected value.[14] The ^{1}H NMR spectra of the products **2–5** also confirm that the hydride ligand bridges the metal centers for these compounds; in all cases the hydride signals are observed between −18.4 and −18.9 ppm and can be analyzed as an overlapping triplet of quintets with $^1J_{Rh-H} = 20$ Hz and $^2J_{P-H} = 10$ Hz, as expected for a hydrogen atom that is coupled to two chemically equivalent rhodium nuclei and four chemically equivalent phosphorus nuclei. The phenyl and methylene hydrogen resonances of the DPM groups are as usually observed when these groups bridge two metals;[15-17] in particular the latter appear as an AB quartet, due to the inequivalence of the methylene hydrogens. and are further split into quintets due to virtual coupling t all four phosphorus nuclei. The $^{31}P\{^1H\}$ NMR spectra for all compounds are also consistent with the above results and display a symmetrical pattern typical of an AA′A″A‴XX′ spin system. These spectra, an example of which is shown in the supplementary data, are dominated by two major peaks, which are separated by ca. 95 Hz. Analyses of similar spectra by Mague and co-workers[18] have suggested that this separation is essentially that of $^1J_{Rh-P}$ and on the basis of our previous observations suggests the presence of a Rh–Rh bond.[19]

A detailed examination of the reaction of **1** with HCl allows us to establish the structure of this product and further enables us to suggest structures for the products in the other protonation reactions and to rationalize the spectral parameters on the basis of these proposed structures. The reaction of **1** with anhydrous HCl in scrupulously dry CH_2Cl_2 yields, upon crystallization, $[Rh_2Cl_3(\mu\text{-}H)(\mu\text{-}CO)(DPM)_2]$ (**2b**) as a yellow powder. However in the presence of any moisture, either through use of technical grade HCl or inadequately dried solvents, the closely related species $[Rh_2Cl_3(\mu\text{-}H)(\mu\text{-}CO)\text{-}(DPM)_2]\cdot H_2O$ (**2a**) can be isolated as a yellow-orange powder. All spectroscopic properties for **2a** and **2b** are very similar apart from the O–H stretches due to H_2O that are present in the infrared spectrum of **2a**. These appear as a sharp band at 3657 cm^{-1} and a broad one at 3436 cm^{-1}. In water molecules in which there is no hydrogen bonding a difference of ca. 100 cm^{-1} is observed between the antisymmetric and symmetric O–H stretching frequencies.[20] The larger difference (221

(8) Cromer, D. T.; Waber, J. T. "International Tables for X-ray Crystallography"; Kynoch Press: Birmingham, England, 1974; Vol. IV, Table 2.2A.
(9) Stewart, R. F.; Davidson, E. R.; Simpson, W. T. *J. Chem. Phys.* **1965**, *42*, 3175–3187.
(10) Cromer, D. T.; Liberman, D. *J. Chem. Phys.* **1970**, *53*, 1891–1898.
(11) $R = \sum||F_o| - |F_c||/\sum|F_o|$; $R_w = [\sum w(|F_o| - |F_c|)^2/\sum wF_o^2]^{1/2}$.
(12) Supplementary material.
(13) Kaesz, H. D.; Saillant, R. B. *Chem. Rev.* **1972**, *72*, 231–281.
(14) Schunn, R. A. "Transition Metal Hydrides"; Muetterties, E. L., Ed.; Marcel Dekker: New York, 1971; Vol. 1, 203–269.
(15) McKeer, I. R.; Cowie, M. *Inorg. Chim. Acta* **1982**, *65*, L107–L109.
(16) Balch, A. L.; Benner, L. S.; Olmstead, M. M. *Inorg. Chem.* **1979**, *18*, 2996–3003.
(17) Balch, A. L.; Hurt, C. T.; Lee, C.-L.; Olmstead, M. M.; Farr, J. P. *J. Am. Chem. Soc.* **1981**, *103*, 3764–3772.
(18) Mague, J. T.; DeVries, S. H. *Inorg. Chem.* **1980**, *19*, 3743–3755.
(19) Typically we have observed that in A-frame compounds closely related to the present ones, the splitting between the two major peaks is less than ca. 120 Hz for Rh–Rh-bonded species and greater than this value for species not containing Rh–Rh bonds. Although there is ambiguity near this value, we have yet to encounter a species having a splitting less than 100 Hz that is not Rh–Rh bonded. See for example: Cowie, M.; Dwight, S. K. *Inorg. Chem.* **1980**, *19*, 209, 2500. Cowie, M.; Southern, T. G. *Ibid.* **1982**, *21*, 246. McKeer, I. R.; Cowie, M. *Inorg. Chim. Acta* **1982**, *65*, L107.
(20) Vinogradov, S. N.; Linnell, R. H. "Hydrogen Bonding"; Van Nostrand-Reinhold: New York, 1971, Chapter 3.

Table III. Positional and Equivalent Isotropic Thermal Parameters for the Nongroup Atoms of $[Rh_2C_{13}(\mu\text{-H})(\mu\text{-CO})(DPM)_2]\cdot H_2O$

atom	x[a]	y	z	B, Å^2	atom	x	y	z	B, Å^2
Rh(1)	−0.339 71 (2)	0.104 09 (4)	0.041 37 (2)	2.19	P(4)	−0.24571 (8)	−0.07978 (12)	0.10881 (7)	2.53
Rh(2)	−0.308 14 (2)	0.012 09 (4)	0.132 59 (2)	2.29	O(1)	−0.2517 (2)	0.1807 (3)	0.13043 (19)	3.54
Cl(1)	−0.329 93 (9)	0.240 26 (13)	−0.002 89 (7)	3.49	O(2)	−0.4305 (3)	0.1167 (5)	0.3838 (3)	7.90
Cl(2)	−0.257 44 (9)	0.001 97 (14)	0.219 77 (7)	3.74	C(1)	−0.2852 (3)	0.1309 (5)	0.1073 (3)	2.47
Cl(3)	−0.414 08 (8)	0.032 81 (15)	0.472 00 (7)	3.95	C(2)	−0.4432 (3)	0.0963 (5)	0.0967 (3)	3.02
P(1)	−0.413 54 (8)	0.177 40 (13)	0.062 13 (7)	2.68	C(3)	−0.2621 (3)	0.0851 (5)	0.0395 (3)	2.66
P(2)	−0.388 97 (8)	0.053 14 (13)	0.152 44 (7)	2.59	H(1)	−0.348 (3)	0.003 (4)	0.073 (2)	3.1 (15)[b]
P(3)	−0.273 39 (8)	0.027 31 (13)	0.010 57 (7)	2.44					

[a] Estimated standard deviations in the least significant figure(s) are given in parentheses in this and all subsequent tables. [b] This atom was refined isotropically.

Table IV

Derived Parameters for the Rigid-Group Atoms of $[Rh_2Cl_3(\mu\text{-H})(\mu\text{-CO})(DPM)_2]\cdot H_2O$

atom	x	y	z	B, Å^2	atom	x	y	z	B, Å^2
C(11)	−0.3852 (3)	0.1334 (3)	0.2037 (2)	2.69 (14)	C(51)	−0.1704 (2)	−0.0690 (4)	0.13364 (18)	2.83 (14)
C(12)	−0.4274 (3)	0.1380 (3)	0.22698 (19)	3.64 (16)	C(52)	−0.1464 (3)	0.0024 (3)	0.16618 (19)	4.63 (19)
C(13)	−0.4230 (4)	0.1992 (4)	0.2666 (2)	4.43 (19)	C(53)	−0.0884 (3)	0.0090 (3)	0.1859 (2)	6.5 (3)
C(14)	−0.3765 (3)	0.2558 (3)	0.2830 (2)	4.56 (19)	C(54)	−0.0544 (2)	−0.0559 (4)	0.17305 (18)	6.3 (3)
C(15)	−0.3343 (3)	0.2512 (3)	0.25977 (19)	4.16 (18)	C(55)	−0.0785 (3)	−0.1272 (3)	0.14051 (19)	5.2 (2)
C(16)	−0.3387 (4)	0.1900 (4)	0.2201 (2)	3.18 (15)	C(56)	−0.1364 (3)	−0.1338 (3)	0.1208 (2)	4.14 (18)
C(21)	−0.4202 (3)	−0.0490 (3)	0.1699 (2)	3.14 (15)	C(61)	−0.2580 (2)	−0.1947 (3)	0.1276 (2)	2.84 (14)
C(22)	−0.3856 (3)	−0.1080 (5)	0.20527 (17)	5.5 (2)	C(62)	−0.2920 (2)	−0.2568 (4)	0.09405 (16)	3.50 (16)
C(23)	−0.4079 (3)	−0.1859 (4)	0.2205 (2)	7.0 (3)	C(63)	−0.3028 (2)	−0.3416 (3)	0.11170 (17)	4.38 (18)
C(24)	−0.4648 (3)	−0.2047 (3)	0.2004 (2)	6.1 (2)	C(64)	−0.2795 (2)	−0.3641 (3)	0.1629 (2)	3.92 (17)
C(25)	−0.4994 (3)	−0.1457 (5)	0.16512 (17)	6.4 (3)	C(65)	−0.2455 (2)	−0.3020 (4)	0.19652 (16)	4.33 (18)
C(26)	−0.4771 (3)	−0.0679 (4)	0.1499 (2)	5.1 (2)	C(66)	−0.2347 (2)	−0.2173 (3)	0.17887 (17)	3.83 (17)
C(31)	−0.2028 (2)	0.0735 (4)	0.02329 (16)	2.71 (14)	C(71)	−0.4713 (3)	0.2158 (4)	0.00870 (18)	3.20 (15)
C(32)	−0.1904 (2)	0.1615 (4)	0.04198 (18)	3.88 (17)	C(72)	−0.5184 (3)	0.1619 (3)	−0.0119 (2)	3.58 (16)
C(33)	−0.1367 (3)	0.1963 (3)	0.0503 (2)	5.3 (2)	C(73)	−0.5611 (3)	0.1923 (4)	−0.05409 (16)	5.3 (2)
C(34)	−0.0954 (2)	0.1430 (4)	0.04000 (16)	5.5 (2)	C(74)	−0.5566 (3)	0.2766 (4)	−0.07563 (18)	5.6 (2)
C(35)	−0.1079 (2)	0.0550 (4)	0.02131 (18)	5.6 (2)	C(75)	−0.5095 (3)	0.3305 (3)	−0.0550 (2)	5.4 (2)
C(36)	−0.1616 (3)	0.0203 (3)	0.0130 (2)	4.52 (19)	C(76)	−0.4669 (3)	0.3001 (4)	−0.01284 (16)	4.37 (18)
C(41)	−0.2944 (2)	0.0034 (4)	−0.05789 (15)	2.69 (13)	C(81)	−0.4006 (3)	0.2785 (3)	0.1021 (2)	3.09 (15)
C(42)	−0.2805 (2)	−0.0784 (3)	−0.07659 (18)	3.48 (16)	C(82)	−0.3514 (2)	0.3284 (4)	0.1105 (2)	4.37 (18)
C(43)	−0.2956 (2)	−0.0936 (3)	−0.1290 (2)	4.37 (18)	C(83)	−0.3428 (2)	0.4060 (4)	0.1408 (2)	6.3 (2)
C(44)	−0.3247 (2)	−0.0270 (4)	−0.16268 (15)	4.38 (18)	C(84)	−0.3833 (3)	0.4338 (3)	0.1629 (2)	6.9 (3)
C(45)	−0.3386 (2)	0.0548 (3)	−0.14398 (18)	4.24 (18)	C(85)	−0.4325 (2)	0.3839 (4)	0.1546 (2)	6.1 (2)
C(46)	−0.3235 (2)	0.0700 (3)	−0.0916 (2)	3.49 (16)	C(86)	−0.4412 (2)	0.3063 (4)	0.1242 (2)	4.40 (19)

Rigid-Group Parameters

	x_0[a]	y_0	z_0	δ[b]	ϵ	η
ring 1	−0.380 86 (14)	0.1946 (2)	0.243 38 (13)	3.909 (3)	0.714 (5)	1.114 (4)
ring 2	−0.442 53 (18)	−0.1269 (3)	0.185 19 (15)	0.540 (4)	2.930 (5)	1.860 (4)
ring 3	−0.149 13 (16)	0.1083 (3)	0.031 64 (13)	0.501 (4)	0.286 (4)	2.739 (3)
ring 4	−0.309 57 (14)	−0.0118 (2)	0.110 28 (13)	−0.407 (3)	1.907 (3)	2.966 (3)
ring 5	−0.112 42 (17)	−0.0624 (3)	0.153 34 (14)	3.727 (4)	−0.028 (4)	3.059 (4)
ring 6	−0.268 77 (14)	−0.2794 (2)	0.145 29 (13)	3.527 (3)	2.094 (4)	4.976 (3)
ring 7	−0.513 98 (16)	0.2462 (3)	−0.033 46 (14)	0.448 (4)	2.618 (4)	3.506 (4)
ring 8	−0.391 97 (17)	0.3562 (3)	0.132 53 (14)	0.590 (4)	0.549 (4)	4.875 (4)

[a] X_0, Y_0, and Z_0 are the fractional coordinates of the centroid of the rigid group. [b] The rigid-group orientation angles δ, ϵ, and η (radians) are the angles by which the rigid body is rotated with respect to a set of axes X, Y, and Z. The origin is the center of the ring: X is parallel to a^*, Z is parallel to c, and Y is parallel to the line defined by the intersection of the plane containing a^* and b^* with the plane containing b and c.

cm^{-1}) between the bands and the broadness of the lower frequency band in the present case suggest that this band results from an O–H which is involved in hydrogen bonding while the 3657-cm^{-1} band corresponds to the free O–H stretch. Consistent with this interpretation, the X-ray structure determination of **2a** confirms that the water molecule is within hydrogen-bonding distance of one of the chloro ligands (vide infra).

The ^{1}H and ^{31}P{^{1}H} NMR data for compound **2** suggest a symmetrical structure as we had expected for the simple protonation of the Rh–Rh bond. However, the conductivity measurement of this species, which shows that **2** is a nonelectrolyte, instead suggests a structure in which the chloride counterion is coordinated to the metal, as is observed in the solid-state structure of **2a** (vide infra). The infrared spectra of the solid and solution are also virtually identical, arguing in favor of similar structures; it would be expected that a cationic species resulting from Cl$^-$ loss would have a significantly different carbonyl stretch.

Although the ^{31}P{^{1}H} NMR spectra in the presence of excess HCl show no obvious change on lowering the temperature from +25 to −80 °C, significant changes are observed in the absence of excess acid. A ^{31}P{^{1}H} NMR spectrum run at 25 °C without excess HCl present appears essentially identical with those run in excess HCl; however, at −80 °C the two major peaks have coalesced into one broad one. Similarly, the well-resolved hydride and DPM methylene hydrogen resonances broaden into unresolved resonances in the absence of excess HCl at −80 °C. Clearly a fluxional process is occurring in solution. The infrared spectrum of this solution also shows a new carbonyl band at 1764 cm^{-1}, which appears as about 10% of that due **2a** (at 1818 cm^{-1}). This new band can be assigned to the unprotonated starting material **1** and can be made to disappear by the addition of HCl. The ^{31}P{^{1}H} and ^{1}H resonances again

sharpen at −80 °C upon HCl addition. We therefore suggest that the fluxionality observed is as diagrammed

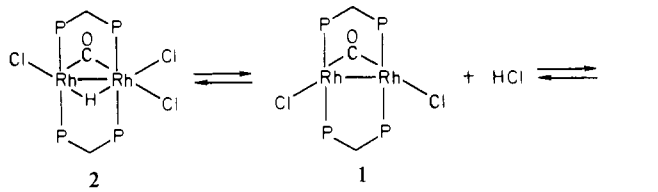

2 1

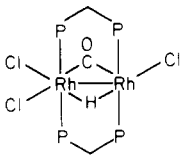

2

Further support for this process can be seen on mixing **2a** and **1** (in a 5:1 ratio by weight) in CH_2Cl_2; the resulting $^{31}P\{^1H\}$ NMR spectrum shows only a single averaged pattern similar to that of **2a** (only broader) at 21.1 ppm with $J \approx 96 \pm 5$ Hz. The chemical shift is essentially what we would expect on the basis of the mole fractions of **1** and **2a** (although the coupling constant is not the weighted average, this resonance is rather broad and the magnitude of the splitting cannot be accurately established). Subsequent additions of more compound **1** to the solution cause an increase in the splitting between the two major peaks and a change in the chemical shift toward that of **1**. The above exchange can be seen to average both Rh and all four phosphorus environments such that in the NMR spectra resonances characteristic of symmetrical species are obtained. In addition, the above process is also consistent with the observed broadening of the ^1H signal due to loss of the Rh–H and P–H coupling in the unprotonated extreme. Attempts to determine the effect of excess chloride ion on the fluxional process through the addition of $NMe_4^+Cl^-$ were unsuccessful since solvents in which this salt is sufficiently soluble resulted in deprotonation of compound **2**.

The reaction of **1** with *p*-toluenesulfonic acid proceeds in a fashion analogous to that for HCl, yielding $[Rh_2Cl_2(\mu\text{-}H)(\mu\text{-}CO)(DPM)_2(O_3SC_6H_4CH_3)]$ (**3**). In addition to the Rh–H and C–O stretches at 1261 and 1806 cm^{-1}, respectively, which again confirm that the hydride and carbonyl ligands bridge the metals, the solid-state infrared spectrum of **3** displays three strong bands at 1231, 1152, and 998 cm^{-1}, typical of S–O stretches for a sulfonate group that is coordinated through one of its oxygen atoms;[21] in the free anion the S–O stretches are near 1290 and 1120 cm^{-1}. In solution the infrared spectrum is very similar to that in the solid, apart from a weak band due to the carbonyl stretch of **1**. Like compound **2**, the *p*-toluenesulfonate derivative is essentially nonconducting in CH_2Cl_2 and has ^1H and $^{31}P\{^1H\}$ NMR parameters very similar to those of **2**; again the resonances, which suggest a symmetrical species, are sharp at all temperatures between +25 and −80 °C in the presence of excess acid but broaden and coalesce at low temperature in the absence of excess acid. These very close similarities in spectral properties suggest that the structure of **3** in the solid is much like that of **2** but with a coordinated *p*-toluenesulfonate group instead of a chloro ligand, as shown. Furthermore, this is probably the predominant solution species which is fluxional by much the same process as was suggested for **2** (vide supra) through reversible loss of *p*-toluenesulfonic acid.

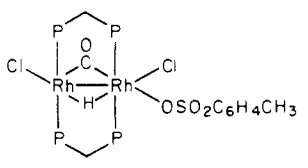

3

The reaction of **1** with $HBF_4 \cdot Et_2O$ also yields a species that we propose is analogous to that diagrammed for the *p*-toluenesulfonate derivative, but with BF_4^- replacing $O_3SC_6H_4CH_3^-$. This species, $[Rh_2Cl_2(\mu\text{-}H)(\mu\text{-}CO)(DPM)_2(BF_4)]$ (**4**), is isolated as the methylene chloride solvate and again shows spectral parameters similar to those for compounds **2** and **3**. Although it was initially surprising to find that the BF_4^- anion was coordinated to one rhodium center, such complexes are known.[21-23] The coordination of the BF_4^- group can be seen clearly in the infrared spectrum of **4** where the strong band normally observed for the free BF_4^- anion at ca. 1055 cm^{-1} is replaced by three weak ones at 1170, 1069, and 984 cm^{-1}. Such a three-band pattern has been observed in other compounds in which BF_4^- coordinates to a metal through one of its fluorine atoms[21-23] and can be attributed to a lowering of the local symmetry of the BF_4^- group from T_d to C_{3v} on coordination, causing three infrared-active B–F stretches (2 A_1 + E) to appear. It has been further suggested that the frequency difference between bands due to coordination and free BF_4^- reflects the amount that the B–F bonding is perturbed; for the lowest lying A_1 band this shows the weakening of the B–F bond due to the competing Lewis acidity of the metal.[22] So in complexes where BF_4^- is strongly coordinated, such as $(\eta^5\text{-}C_5H_5)(CO)_3MoBF_4$,[22] the splitting is large, and for this species the B–F stretches appear at 1130, 884, and 722 cm^{-1}. The values observed in the present case are much closer to those in free BF_4^- and suggest weak coordination of this group.

In solution, compound **4** gives rise to $^{31}P\{^1H\}$ and ^1H NMR spectra similar to those for compounds **2** and **3**, except that no temperature dependence is observed for **4**, in either the presence or the absence of excess acid. Also unlike those of the previous compounds, the solution infrared spectrum of **4** shows no evidence of the starting compound **1**, suggesting that exchange with free acid, as occurred with **2** and **3**, is not occurring, probably because BF_4^- is such a weak base. The conductivity of **4** is somewhat higher than those of **2** and **3** but is still much less than expected were the BF_4^- anion not associated with the complex.[6] On the basis of these data we propose that the predominant species in solution is the unsymmetrical one having coordinated BF_4^- but that the fluxional process is not occurring by reversible HBF_4 loss analogous to the processes observed for compounds **2** and **3**. We suggest instead that this fluxional process occurs through exchange of coordinated and free BF_4^-:

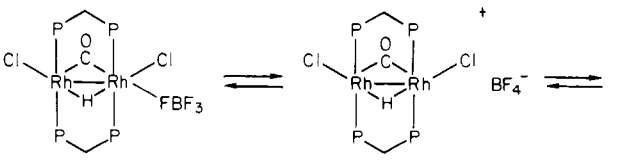

4

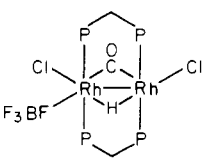

4

(21) Olgemöller, B.; Bauer, H.; Beck, W. *J. Organomet. Chem.* **1981**, *213*, C57–C59.

(22) Beck, W.; Schloter, K. *Z. Naturforsch. B: Anorg. Chem., Org. Chem.* **1978**, *33B*, 1214–1222.

(23) Beck, W.; Schloter, K. *Z. Naturforsch., B: Anorg. Chem., Org. Chem.* **1980**, *35B*, 985–989.

Table V. Selected Interatomic Distances (Å) in $[Rh_2Cl_3(\mu\text{-}H)(\mu\text{-}CO)(DPM)_2]\cdot H_2O$

Bond Distances							
Rh(1)-Rh(2)	2.7464 (7)	Rh(2)-C(1)	2.026 (7)	P(1)-C(2)	1.816 (7)	P(2)-C(11)	1.819 (4)
Rh(1)-Cl(1)	2.393 (2)	Rh(1)-P(1)	2.355 (2)	P(2)-C(2)	1.828 (7)	P(2)-C(21)	1.824 (5)
Rh(1)-Cl(3)	2.462 (2)	Rh(1)-P(3)	2.366 (2)	P(3)-C(3)	1.818 (7)	P(3)-C(31)	1.826 (4)
Rh(2)-Cl(2)	2.358 (2)	Rh(2)-P(2)	2.329 (2)	P(4)-C(3)	1.825 (7)	P(3)-C(41)	1.829 (4)
Rh(1)-H(1)	1.76 (6)	Rh(2)-P(4)	2.305 (2)	P(1)-C(71)	1.813 (4)	P(4)-C(51)	1.809 (4)
Rh(2)-H(1)	1.65 (6)	C(1)-O(1)	1.149 (8)	P(1)-C(81)	1.819 (4)	P(4)-C(61)	1.820 (4)
Rh(1)-C(1)	1.952 (7)						
Nonbonded Distances							
Cl(3)-O(2)	3.204 (7)	Cl(1)-H(46)	2.66	Cl(2)-H(66)	2.88	O(1)-H(82)	2.59
P(1)-P(2)	2.992 (3)	Cl(1)-H(56)[a]	2.78	O(2)-C(2)[b]	3.38 (1)	O(1)-H(32)	2.63
P(3)-P(4)	3.020 (3)	Cl(1)-H(32)	2.79	O(2)-H2C2[c]	2.53	O(1)-H(16)	2.83
Cl(1)-C(1)	3.312 (7)	Cl(1)-H(82)	2.87	O(2)-H(33)[d]	2.55	O(1)-H(52)	2.84
C(2)-H(1)	2.99 (6)	Cl(1)-H(22)	2.63	O(2)-H(26)	2.70	C(1)-H(1)	2.45 (6)
C(3)-H(1)	2.88 (6)	Cl(2)-H(52)	2.92				

[a] Atom located at $\bar{x} - 1/2, 1/2 + y, \bar{z}$. [b] Atom located at $\bar{x} - 1, y, 1/2 - z$. [c] Atom located at $\bar{x} - 1, y, 1/2 - z$. [d] Atom located at $\bar{x} - 1/2, 1/2 - y, 1/2 - z$.

This process results in transfer of BF_4^- from one end of the complex to the other, thereby rendering both rhodium centers equivalent on the NMR time scale. We were unable to look at the effect of added BF_4^- on this equilibrium since solvents in which the BF_4^- salts are soluble resulted in deprotonation of the complex to give compound **1**, as was the case with compound **2**. It should also be noted that such a process, in addition to those proposed to explain the solution spectra of compounds **2** and **3** (vide supra), cannot be ruled out as a competing process in either of these equilibria.

If the reaction between **1** and $HBF_4\cdot Et_2O$ is carried out in THF instead of CH_2Cl_2, a light yellow precipitate immediately forms which analyzes as $[Rh_2Cl_2(\mu\text{-}H)(\mu\text{-}CO)(DPM)_2(THF)][BF_4]$ (**5**). Unfortunately, characterization of **5** in solution has not been possible; it is insoluble in THF, and in other solvents such as CH_2Cl_2 only the starting material **1** is observed unless excess acid is used, in which case only **4** is obtained. The infrared spectrum of a solid sample of **5** has $\nu(CO) = 1785\ cm^{-1}$ and $\nu(Rh\text{-}H) = 1230\ cm^{-1}$, which, although typical for bridging carbonyl and hydride ligands, are significantly different from the values observed for compounds **2–4**, which are all closely comparable. Compound **5** also displays a broad intense band at 1056 cm^{-1} due to free BF_4^-, indicating that this anion is not coordinated to the metals, and a medium-intensity band at 872 cm^{-1} due to coordinated THF. Free THF has two bands at 1068 and 908 cm^{-1}, which shift to lower frequency by ca. 40–100 cm^{-1} upon coordination.[24-26] Although the expected higher frequency band is obscured due to the intense bands of BF_4^- and the DPM ligands, the lower frequency band is clearly observed. These spectral data and the satisfactory elemental analysis indicate that compound **5** has a structure much like those of **3** and **4** but with the $O_3SC_6H_4CH_3^-$ and BF_4^- anions, respectively, replaced by a coordinating THF molecule. Beck has described a series of donor strengths for weakly coordinating ligands and concludes that they increase in the order $CH_2Cl_2 < BF_4^- < THF$.[23] So it is not surprising to observe replacement of the BF_4^- anion by a THF molecule in the inner coordination sphere of compound **5**. The somewhat different carbonyl and metal–hydride stretches for compound **5** compared with those of compounds **2–4** are understandable on the basis of the replacement of anionic groups by a neutral one, although one might naively expect an increase in the carbonyl stretching frequency in **5**, instead of the observed decrease, because of the resulting positive charge on compound **5**. However, THF is more strongly coordinating than BF_4^-, so the more basic THF molecule donates more electron density to the metals with a concomitant lowering of the carbonyl stretching frequency of **5** with respect to **4**. The similarities in the $\nu(CO)$ values in compounds **2–4** also suggest that, like BF_4^-, the Cl^- and $p\text{-}O_3SC_6H_4CH_3^-$ anions are weakly coordinating in these complexes. This is supported by the structure of **2a** which shows one long Rh–Cl bond (vide infra).

Description of the Structure of 2a. Attempted crystallization of compounds **2b**, **3**, and **4** has repeatedly yielded crystals of unsuitable quality for X-ray diffraction studies. Only the HCl adduct, as the H_2O solvate (**2a**), has given suitable crystals.

In the solid state, compound **2a** has a water molecule of crystallization which is associated with one of the chloro ligands (Cl(3)) such that the chlorine–oxygen distance involving this water molecule (Cl(3)–O(2)) is 3.204 (7) Å. Although neither hydrogen atom of this water molecule was located, the Cl(3)–O(2) distance is equal to the sum of the two van der Waals radii[27] and so is not inconsistent with a hydrogen bond between these two atoms. Spectroscopic evidence for hydrogen bonding of the H_2O molecule was observed in the infrared spectrum (vide supra), and presumably it is this interaction that is responsible for the presence of H_2O in the structure. The only other short contacts involving O(2) are with C(2), H(2C4), H(33), and H(26) (see Table V). Although these contacts are shorter than van der Waals contacts, they are not particularly unusual.

We had initially anticipated that the reaction of **1** with HCl would occur in one of two ways: either by simple protonation of the Rh–Rh bond, yielding a cationic complex and a chloro counterion, or by oxidative addition with both the H and Cl ligands bonding terminally (probably with one on each metal). The solid-state structure of the product is neither of those anticipated but is in fact a combination of the Rh–Rh bond protonation product and the oxidative-addition product such that this species has the hydride ligand bridging the two metals and the chlorine atom coordinated to one of the metals (see Figure 1). As a result, the geometries about the two metals differ significantly; if the formal Rh–Rh bond is ignored, the geometry about Rh(1) is that of a slightly distorted octahedron whereas the geometry about Rh(2) is intermediate between a trigonal bipyramid, having C(1), P(2), and P(4) in the equatorial sites, and a tetragonal pyramid with C(1) at the apical site. As a consequence, P(1) and P(3) are almost mutually trans (P(1)–Rh(1)–P(3) = 173.01 (7)°) while P(2) and P(4) are bent significantly about Rh(2) (P(2)–Rh(2)–P(4) = 158.45 (7)°). The deviations from the idealized geometries are also clearly shown in the differences of other angles about Rh(1) and Rh(2) (see Table VI) from their respective idealized

(24) Masino, A. P. Ph.D. Thesis, The University of Alberta, 1978; p 73.
(25) Allan, K. A.; Gowenlock, B. G.; Lindsell, W. E. *J. Organomet. Chem.* **1973**, *55*, 229–235.
(26) Eyster, J. M.; Prohofsky, E. W. *Spectrochim. Acta, Part A* **1974**, *30A*, 2041–2046.
(27) Pauling, L. "The Nature of the Chemical Bond", 3rd ed.; Cornell University Press: Ithaca, NY, 1960; Table 7-20, p 260.

Table VI. Selected Angles (deg) in $[Rh_2Cl_3(\mu\text{-}H)(\mu\text{-}CO)(DPM)_2]\cdot H_2O$

H(1)-Rh(1)-C(1)	82 (2)	H(1)-Rh(2)-C(1)	83 (2)	C(3)-P(3)-Rh(1)	108.0 (2)	C(61)-P(4)-C(3)	104.7 (3)
H(1)-Rh(1)-P(1)	93 (2)	H(1)-Rh(2)-P(4)	86 (2)	C(3)-P(4)-Rh(2)	111.2 (2)	C(61)-P(4)-Rh(2)	106.0 (2)
H(1)-Rh(1)-P(3)	88 (2)	H(1)-Rh(2)-P(2)	87 (2)	C(71)-P(1)-C(2)	106.0 (3)	P(1)-C(2)-P(2)	110.4 (4)
H(1)-Rh(1)-Cl(3)	81 (2)	H(1)-Rh(2)-Cl(2)	169 (2)	C(71)-P(1)-C(81)	100.9 (3)	P(3)-C(3)-P(4)	112.0 (4)
H(1)-Rh(1)-Cl(1)	179 (2)	H(1)-Rh(2)-Rh(1)	38 (2)	C(71)-P(1)-Rh(1)	116.1 (2)	P(1)-C(71)-C(72)	121.6 (3)
H(1)-Rh(1)-Rh(2)	35 (2)	C(1)-Rh(2)-P(2)	102.4 (2)	C(81)-P(1)-C(2)	104.3 (3)	P(1)-C(71)-C(76)	118.3 (3)
Cl(3)-Rh(1)-C(1)	163.5 (2)	C(1)-Rh(2)-P(4)	96.9 (2)	C(81)-P(1)-Rh(1)	120.7 (2)	P(1)-C(81)-C(82)	121.1 (3)
Cl(3)-Rh(1)-P(1)	85.19 (7)	C(1)-Rh(2)-Cl(2)	107.6 (2)	C(11)-P(2)-C(2)	106.1 (3)	P(1)-C(81)-C(86)	118.9 (3)
Cl(3)-Rh(1)-P(3)	88.21 (7)	C(1)-Rh(2)-Rh(1)	45.2 (2)	C(11)-P(2)-C(21)	104.8 (3)	P(2)-C(11)-C(12)	121.3 (3)
Cl(3)-Rh(1)-Cl(1)	97.57 (7)	P(4)-Rh(2)-P(2)	158.45 (7)	C(11)-P(2)-Rh(2)	120.3 (3)	P(2)-C(11)-C(16)	118.7 (3)
Cl(3)-Rh(1)-Rh(2)	116.08 (6)	P(4)-Rh(2)-Cl(2)	91.92 (7)	C(21)-P(2)-C(2)	103.7 (3)	P(2)-C(21)-C(22)	118.0 (4)
C(1)-Rh(1)-P(1)	93.6 (2)	P(4)-Rh(2)-Rh(1)	93.59 (5)	C(21)-P(2)-Rh(2)	108.7 (2)	P(2)-C(21)-C(26)	121.9 (4)
C(1)-Rh(1)-P(3)	93.3 (2)	P(2)-Rh(2)-Cl(2)	91.39 (7)	C(31)-P(3)-C(3)	103.9 (3)	P(3)-C(31)-C(32)	120.8 (3)
C(1)-Rh(1)-Cl(1)	98.8 (2)	P(2)-Rh(2)-Rh(1)	93.16 (5)	C(31)-P(3)-C(41)	103.6 (3)	P(3)-C(31)-C(36)	119.2 (3)
C(1)-Rh(1)-Rh(2)	47.4 (2)	Rh(1)-H(1)-Rh(2)	107 (3)	C(31)-P(3)-Rh(1)	119.9 (2)	P(3)-C(41)-C(42)	121.3 (3)
P(1)-Rh(1)-P(3)	173.01 (7)	Rh(1)-C(1)-Rh(2)	87.3 (3)	C(41)-P(3)-C(3)	103.6 (3)	P(3)-C(41)-C(46)	118.7 (3)
P(1)-Rh(1)-Cl(1)	87.07 (7)	O(1)-C(1)-Rh(1)	146.2 (6)	C(41)-P(3)-Rh(1)	116.4 (2)	P(4)-C(51)-C(52)	120.5 (3)
P(1)-Rh(1)-Rh(2)	92.00 (5)	O(1)-C(1)-Rh(2)	126.5 (6)	C(51)-P(4)-C(3)	106.2 (3)	P(4)-C(51)-C(56)	119.5 (3)
P(3)-Rh(1)-Cl(1)	91.50 (7)	C(2)-P(1)-Rh(1)	107.5 (2)	C(51)-P(4)-C(61)	102.8 (3)	P(4)-C(61)-C(62)	122.9 (3)
P(3)-Rh(1)-Rh(2)	92.98 (5)	C(2)-P(2)-Rh(2)	111.8 (2)	C(51)-P(4)-Rh(2)	124.1 (2)	P(4)-C(61)-C(66)	117.0 (3)
Cl(1)-Rh(1)-Rh(2)	146.15 (5)						

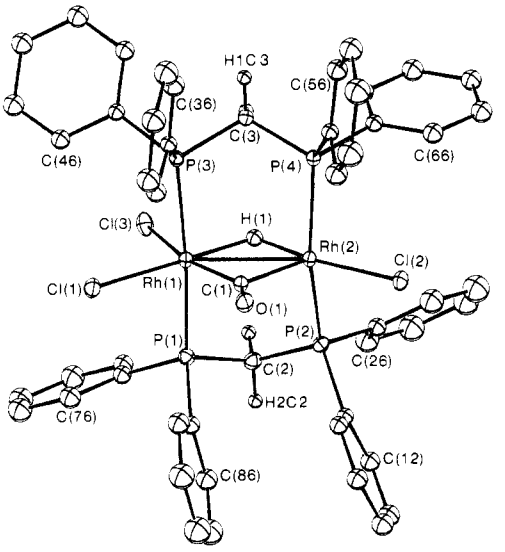

Figure 1. Perspective view of $[Rh_2Cl_3(\mu\text{-}H)(\mu\text{-}CO)(DPM)_2]$ showing the numbering scheme. Phenyl rings are numbered sequentially around each ring starting at the carbon bound to phosphorus; phenyl hydrogen atoms have the same number as their attached carbon atom. 20% thermal ellipsoids are shown in both figures, with the exception of the methylene hydrogen atoms which are drawn artificially small.

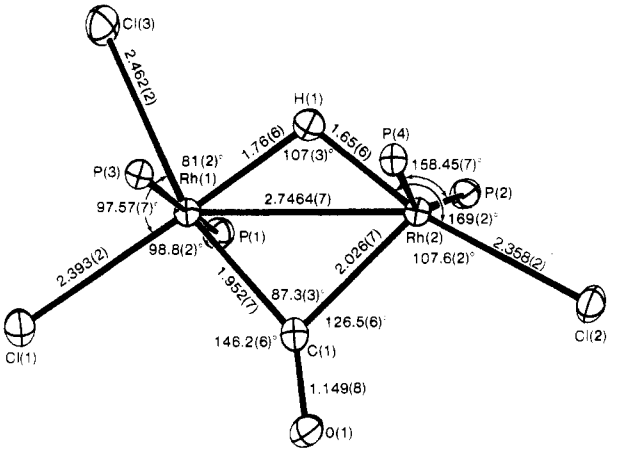

Figure 2. Inner coordination sphere of $[Rh_2Cl_3(\mu\text{-}H)(\mu\text{-}CO)(DPM)_2]$ showing some relevant parameters. In addition the P(1)–Rh(1)–P(3) angle is 173.01 (7)°.

values. The geometries about Rh(1) and Rh(2) can be clearly seen in Figure 2, which shows the inner coordination sphere.

Within the rhodium–DPM framework most parameters are normal for such a dimer.[1,5,28-33] However, there is a significant range in the Rh–P distances (2.305 (2)–2.366 (2) Å) with the shortest two being associated with Rh(2). It may be that P(1) and P(2), which are mutually trans, exert a larger trans influence on each other than do P(2) and P(4), which are bent significantly from being trans. More likely however, the more severe steric congestion about Rh(1) causes a lengthening of these Rh–P bonds due to mutual repulsion between the ligands on this metal center. A similar disparity in Rh–P distances was observed in $[Rh_2Cl(CNMe)_2(CF_3C_2CF_3)(DPM)_2]^+$[34] and in $[Rh_2Cl_2(CO)(SCNMe_2)(DPM)_2]^+$,[35] and again the larger values were associated with the more sterically crowded metal centers.

Surprisingly, the two Rh–Cl bonds (Rh(1)–Cl(1) and Rh(2)–Cl(2)) that are trans to H(1) are not as long as might be expected on the basis of the trans influence of the hydride ligand. These distances (2.393 (2) and 2.358 (2) Å, respectively) are comparable to normal terminal Rh–Cl distances in other related species.[5,36,37] In contrast, the Rh(1)–Cl(3) bond (2.462 (2) Å), which is trans to the carbonyl group, is significantly longer than the other two Rh–Cl distances. It may be that this is the chlorine that is exchanged via HCl loss in solution (vide supra).

The bridging hydride ligand in this structure is well-behaved crystallographically, and the resulting Rh–H distances are essentially as expected and do not differ significantly from each other. The bridging carbonyl group, on the other hand, is somewhat asymmetrically bonded, being significantly closer to Rh(1). As is typically observed in asymmetrically bonded carbonyls,[38] it is also more linear with respect to this rhodium atom (see Figure 2). This asymmetry is probably steric in origin, and it points out the close correspondence between steric and electronic factors in bonding. The increased crowding about Rh(1), owing to the extra chloride ligand (Cl(3)), forces Cl(1) toward the carbonyl groups. This results in close con-

(28) Cowie, M.; Dwight, S. K. *Inorg. Chem.* **1980**, *19*, 2508–2513.
(29) Cowie, M. *Inorg. Chem.* **1979**, *18*, 286–292.
(30) Cowie, M. Dwight, S. K. *Inorg. Chem.* **1979**, *18*, 2700–2706.
(31) Cowie, M.; Dwight, S. K. *Inorg. Chem.* **1980**, *19*, 209–216.
(32) Cowie, M.; Dwight, S. K. *J. Organomet. Chem.* **1981**, *214*, 233–252.
(33) Cowie, M.; Dickson, R. S. *Inorg. Chem.* **1981**, *20*, 2682–2688.
(34) Dickson, R. S.; Hames, B. W.; Cowie, M., submitted for publication.
(35) Gibson, J. A. E.; Cowie, M. *Organometallics*, in press.
(36) Cowie, M.; Dwight, S. K. *Inorg. Chem.* **1981**, *20*, 1534–1538.
(37) Mague, J. T. *Inorg. Chem.* **1969**, *8*, 1975–1981.
(38) Cotton, F. A. Prog. *Inorg. Chem.* **1976**, *21*, 1–28.

tacts of Cl(1) with the ortho hydrogens H(32) and H(82) (2.79 and 2.87 Å, respectively) and of O(1) with these same hydrogens (2.63 and 2.59 Å) forcing O(1) toward Cl(2). By comparison, the closest oxygen–hydrogen contact on the other side is O(1)–H(16) at 2.83 Å, and the closest Cl(2)–hydrogen contact, with H(66), is 2.88 Å. The bending of the carbonyl group as shown tends to increase the σ contribution, with Rh(1) shortening the Rh(1)–C(1) bond. The extreme case of bending would have this carbonyl ligand terminally bound to Rh(1) and side-on bound to Rh(2), as was observed in $[Mn_2(CO)_5(DPM)_2]$.[39] However, we are far from this extreme in the present case since the Rh(2)···O(1) distance, at 2.862 (5) Å, places these atoms outside of bonding distance. In the manganese compound the oxygen of the side-on-bound carbonyl group is only 0.28 Å further from the metal than the carbon atom whereas in the present compound O(1) is almost 0.84 Å further from Rh(2) than is C(1).

The Rh–Rh separation is consistent with a Rh–Rh single bond. As such, it is significantly shorter than the intraligand P···P separation (average 3.01 Å), indicating compression along the Rh–Rh axis and Rh–Rh attraction. Surprisingly, protonation of the metal–metal bond does not seem to have lengthened this bond as judged by comparison with the bromo analogue of the unprotonated precursor.[28] However, the additional effect of Cl^- coordination on the Rh–Rh distance is uncertain, so the effect of protonation on the Rh–Rh distances without anion coordination is not known.

Conclusions

We had originally anticipated that reaction of **1** with acids (HA) would occur either by simple protonation of the Rh–Rh bond or by oxidative addition, yielding a product having H and A each terminally coordinated to different metal centers. Oxidative addition in similar binuclear complexes of rhodium and iridium has already been observed to occur such that the two fragments add to each end of these complexes.[40–43] It seemed reasonable to expect that the former reaction might occur for acids having anions that were only weakly coordinating (e.g. HBF_4) whereas the latter might occur for acids such as HCl. We have in fact found that the acids, HCl, $HSO_3C_6H_4CH_3$, and $HBF_4{\cdot}Et_2O$, all yield similar products and that these products present an interesting variation on the above two possibilities. The structure observed for the HCl adduct (and assumed to be similar for the others) has the Cl^- anion coordinated to one metal but the hydrido group bridging the two metals. This oxidative-addition product is only very subtly different from the one with H and Cl terminally coordinated to each metal. This latter product would, on the basis of electron-counting arguments, have yielded a "ketonic" carbonyl species having no accompanying Rh–Rh bond. On the basis of the paucity of such species, we are led to believe that the factors which stabilize these species in preference to metal–metal-bonded species are subtle, and the structure observed for the present HCl adduct, having a bridging hydrido ligand, is favored owing in part to the retention of the Rh–Rh bonding interaction.

The structure of the HCl adduct (**2a**) also has some interesting implications regarding metal–metal bond protonations in related binuclear complexes. It is our contention that had simple Rh–Rh bond protonation occurred in compound **1**, without additional anion coordination, the structure of the product would be very similar to that observed in **2a** but without Cl(3). We propose therefore that protonation of **1** is accompanied by a change in the configuration of the chloro ligands such that they are no longer trans (or pseudotrans) to the bridging carbonyl group but are now trans to the hydrido ligand (much as Cl(1) and Cl(2) are in compound **2a**). Although it is difficult to argue this point regarding the configuration of ligands about Rh(1) owing to the additional Cl atom (we assume Cl(3)), Rh–Rh bond protonation has obviously caused a significant change in the position of Cl(2), much as we propose. A very similar ligand arrangement is observed in $[Rh_2(CO)_2(\mu\text{-}H)(\mu\text{-}CO)(DPM)_2]^+$, which can be formed by protonation of the neutral tricarbonyl A-frame precursor.[44] Such proposed changes of configuration of the A-frame raise an interesting point concerning the relative preference of ligands to occupy the apical site instead of the enclosed bridging site in doubly bridged A-frames. This transformation would seem to be electronically, as opposed to sterically, induced owing to the small steric bulk of the hydride ligand and has some important chemical implications. If the carbonyl group were at the apex of the A-frame and the hydride ligand were in the enclosed site (structure I) instead of the structure that we propose (structure II), the hydride ligand would be protected from interactions with other substrate molecules, whereas in structure II the hydride ligand is exposed and available for substrate interactions via coordination of the substrate at the adjacent open coordination sites on each metal. Such an arrangement is important if one is to utilize such species in reactions involving the hydride ligand (e.g. hydrogenations, hydroformylations, etc.). We have already seen ligand coordination at one of these open sites in compound **2a** where Cl^- occupies this site and have observed replacement of the weakly coordinating BF_4^- group by THF. It is possible that other coordinating groups such as olefins can also displace the more weakly coordinating ones and in so doing might lead to reactivity of this hydride ligand. We are presently pursuing this point of view in order to determine the reactivities of these hydride species.

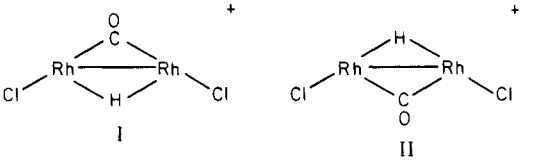

I II

Acknowledgment. The authors thank the University of Alberta and the Natural Sciences and Engineering Research Council of Canada for financial support, the NSERC for a graduate scholarship to B.R.S. and Professor J. Takats for helpful discussions.

Registry No. **1**, 73680-37-2; **2a**, 89043-33-4; **2b**, 89103-88-8; **2b**-d_1, 89043-34-5; **3**, 89043-35-6; **4**, 89043-36-7; **5**, 89043-38-9; Rh, 7440-16-6; deuterium, 7782-39-0.

Supplementary Material Available: Listings of the idealized hydrogen positional and isotropic thermal parameters, anisotropic thermal parameters, and the observed and calculated structure amplitudes for compound **2a** and a $^{31}P\{^1H\}$ NMR spectrum of compound **3** (21 pages). Ordering information is given on any current masthead page.

(39) (a) Colton, R.; Commons, C. J.; Hoskins, B. F. *J. Chem. Soc., Chem. Commun.* **1975**, 363–364. (b) Commons, C. J.; Hoskins, B. F. *Aust. J. Chem.* **1975**, *28*, 1663–1672.
(40) Balch, A. L.; Tulyathan, B. *Inorg. Chem.* **1977**, *16*, 2840–2845.
(41) Balch, A. L.; Labadie, J. W.; Delker, G. *Inorg. Chem.* **1979**, *18*, 1224–1227.
(42) Sutherland, B. R.; Cowie, M., unpublished results.
(43) McKeer, I. R.; Cowie, M., unpublished results.
(44) Kubiak, C. P.; Woodcock, C.; Eisenberg, R. *Inorg. Chem.* **1982**, *21*, 2119–2129.